

Resonant tunneling in magnetic fields: Evidence for space-charge buildup

V. J. Goldman and D. C. Tsui

Department of Electrical Engineering, Princeton University, Princeton, New Jersey 08544

J. E. Cunningham

AT&T Bell Laboratories, Holmdel, New Jersey 07733

(Received 20 November 1986)

The standard model of double-barrier resonant tunneling structures inadequately describes the experimental current-voltage curves. When applied to experiments on resonant tunneling in quantizing magnetic fields, it leads to incorrect values of the electron effective mass in the well. We show that the space-charge formation, both in the electrodes and in the well, not considered previously, is, in fact, very important. We present a model which takes into account these effects. The calculations, based on our model, are in good agreement with the experimental results.

Presently, there is substantial interest in the physics and device applications of semiconductor-based double-barrier resonant tunneling structures (DBRTS's).¹⁻⁴ The original Tsu-Esaki picture of the DBRTS as a Fabry-Perot resonator for electrons was developed further by Ricco and Azbel.⁵ In this essentially one-dimensional approach a beam of monoenergetic electrons is incident upon the potential profile created by the conduction-band (CB) bottom of a DBRTS. The resonant enhancement of the transmission coefficient occurs when the incident electron energy coincides with the bottom of the subband in the well, E_0 .⁶ As a practical means to observe this phenomenon Tsu and Esaki proposed to dope heavily the regions on both sides of the DBRTS thus creating the emitter and collector electrodes. They assumed that if a bias voltage V is applied to the emitter and the collector the current peak occurs when the bottom of the subband approaches the Fermi level E_F of the emitter and that the bottom of the well shifts by one-half of the voltage for a symmetrical DBRTS (Fig. 1).

Recently, however, it has been pointed out by Luryi³ that the negative differential resistance (NDR) observed in DBRTS's can be explained as due solely to the tunneling of electrons from the three-dimensional states in the

emitter to the two-dimensional (2D) states in the well. Subsequently, the electrons leave the well by tunneling through the collector barrier. In this latter picture, the current through a DBRTS starts to rise when the bottom of the subband coincides with the emitter E_F , continues to rise as the bias is increased, and then drops suddenly when the bottom of the subband is biased just below the CB bottom of the emitter since the component of the electron momentum transverse to the direction of tunneling is conserved. This more realistic approach to the electron transport in the DBRTS is supported by the experimental observation of the NDR in tunneling through a single barrier into a quantum well.²

The experimental I - V curves, however, differ appreciably from those expected in either approach. E_F and E_0 calculated from the experimental data are significantly greater than those calculated from the dimensions and compositions of the DBRTS, using simple quantum mechanics. In the presence of a quantizing magnetic field B , oscillations due to Landau levels in the well are observable.⁴ In this Rapid Communication we report a systematic study of this effect; our data, if analyzed within the standard model, give the electron effective mass m^* a factor of 2 smaller than its true value. Then we present a picture of the DBRTS which takes into account, self-consistently, the space-charge layers formed in the electrodes of a biased device as well as the quite substantial electron population in the well. A simplified model calculation gives results in good agreement with experiment.

Our DBRTS's were grown on an n^+ (100) GaAs substrate and have a 56-Å GaAs well sandwiched between two 85-Å-thick $\text{Al}_{0.40}\text{Ga}_{0.60}\text{As}$ barriers. The GaAs emitter and collector regions were doped with Si to $N_D = 2 \times 10^{17} \text{ cm}^{-3}$. The devices were defined by 110- μm -diam Au-Ni-Ge Ohmic contacts which served as masks for mesa etching.⁷ The I - V characteristics (Fig. 1)⁸ of the device reported here display a current peak-to-valley ratio exceeding 13:1 at 77 K and 17:1 at 4.2 K, the highest values reported for a DBRTS, to our knowledge. This indicates the high purity of the barriers and the quality of the interfaces.

The differential conductance dI/dV of the device was

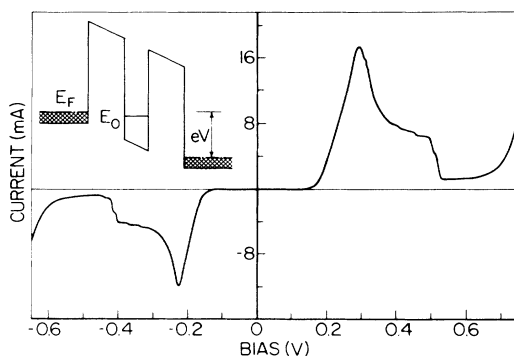


FIG. 1. The I - V curve of the $\text{Al}_x\text{Ga}_{1-x}\text{As}/\text{GaAs}$ DBRTS's at 4.21 K. The CB energy diagram is shown in the inset.

measured using the conventional ac technique with a modulation voltage of 0.5 mV rms. The lowest trace in Fig. 2(a) shows dI/dV as a function of V at 4.21 K and $B=0$. At small biases $V < 0.1$ V, the dI/dV is extremely small. It rises at the onset of tunneling, and as the bias is increased further, remains approximately constant and then drops sharply corresponding to a roughly triangular I - V curve. An instability of the device can be seen at the high-bias end of the trace. When a quantizing B is applied perpendicular to the interface planes the dI/dV curve displays oscillations as a function of V . Alternatively, oscillations can be seen in dI/dV vs B curves at fixed biases [Fig. 2(b)].

The origin of the oscillations is quite clear.⁴ The magnetic field induces Landau quantization of the 2D electronic states in the well so that the density of states peaks at the allowed values of energy, $E_0 + \hbar\omega_c(N + \frac{1}{2})$, as measured from the bottom of the well, where $\omega_c = eB/m^*c$ is the cyclotron frequency and $N=0,1,\dots$ is the Landau index. At a fixed B , as the bias is increased, the resonant tunneling sets in when the energy of the $N=0$ level in the well matches E_F in the emitter. As V is increased further, the tunneling current does not change rapidly until the next Landau level crosses E_F in the emitter. This process continues until the $N=0$ level passes the bottom of the emitter CB. For higher V , direct tunneling is no longer possible due to the conservation of the transverse component of the momentum (i.e., the conservation of Landau index in the presence of B). The steps in the I - V curve translate into peaks in the dI/dV vs V dependence. In GaAs the electron effective g factor is sufficiently small to neglect the spin splitting of the Landau levels. The broadening effects are significant, however, and they are expected to lead to the dI/dV vs V curves shown in Fig. 2(a). The case when V is fixed to a value at which the resonant tunneling takes place and B is raised from $B=0$ is similar and the only major difference is that the $N=0$ Landau level does not cross E_F in the emitter.⁹

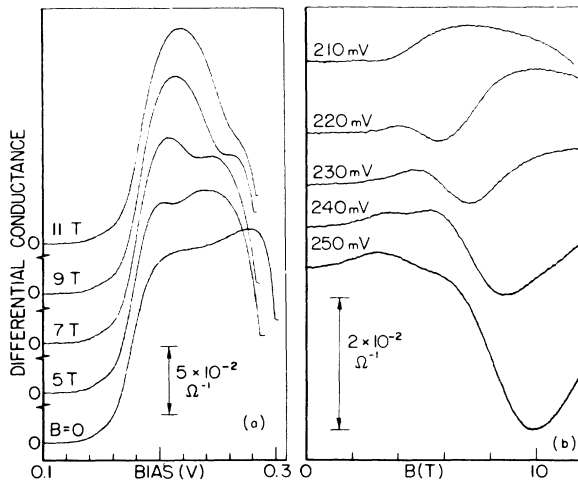


FIG. 2. Differential conductance dI/dV of the DBRTS device (a) as a function of bias V (B fixed) and (b) as a function of magnetic field B (V fixed).

Figure 3(a) gives the fan diagrams of the positions of the maxima (integers) and the minima (half-integers) of the oscillations for both bias polarities. A least-squares fit gives m^* of electrons with energies just above the bottom of the subband in the well. In this fit we used the assumption that the bottom of the well shifts under the bias by $\frac{1}{2}eV$.^{4,5} The obtained $m^* \sim 0.03m_e$ is about a factor of 2 smaller than expected, and, surprisingly, the difference between the values of m^* for the positive and the negative V (Ref. 8) far exceeds the experimental uncertainty.

These discrepancies have led us to reexamine the physics of the DBRTS under bias. Simple estimates show that two previously neglected effects are quite substantial in practically all experimentally studied DBRTS's. The first is the formation of the accumulation and depletion layers¹⁰ in the emitter and the collector electrodes, respectively, in the biased device [Fig. 3(b)]. The areal concentration of electrons and ionized donors is $\sim 5 \times 10^{11} \text{ cm}^{-2}$. The depletion layer reduces the electric field in the barriers and the well thus increasing the bias required to align E_0 and E_F . The accumulation layer lowers the CB edge in the emitter close to the barrier, thus lowering E_0 , relative to E_F , in contrast to the depletion layer, and also extends the range of energies from which the electrons can tunnel.

The second phenomenon is the formation of the space charge created by the tunneling electrons in the well. Once an electron has tunneled into the well it occupies a resonant state with kinetic energy of just above E_0 . If we denote the transmission coefficient of the collector barrier as T_2 , then the lifetime in the well is $\tau \approx \hbar/T_2E_0$. Since the number flux of electrons passing through the well in the steady state is $-J/e$, where J is the tunneling current density, the areal concentration of the electrons in the well is $n_w \approx \hbar J/eT_2E_0$, and the areal space-charge density in the well is

$$-\Sigma \approx -\hbar J/T_2E_0. \quad (1)$$

Consequently, the electric field in the collector barrier V_2/d is appreciably greater than V_1/d [see Fig. 3(b)]. A simple estimate gives $n_w \sim 1 \times 10^{11} \text{ cm}^{-2}$.

We now proceed to the equations describing the processes in the DBRTS at low temperatures. First of all, we note that the voltage drops across the different regions of the structure add up to the applied bias:

$$eV = e(V_1 + V_2 + V_w) + \Delta_1 + \Delta_2 + E_F. \quad (2)$$

Next we consider the accumulation layer in the emitter. The Poisson equation for this region is a 2D Thomas-Fermi nonlinear differential equation which can be solved only numerically.¹¹ We use a simplification in which the electrostatic potential changes linearly across δ_1 and the resulting electric field is equal to that in the emitter barrier:

$$\Delta_1/\delta_1 \approx eV_1/d. \quad (3)$$

The areal charge density required to produce this electric field is

$$\sigma \approx (\epsilon/4\pi)(V_1/d), \quad (4)$$

where ϵ is the static dielectric constant of GaAs. Since σ

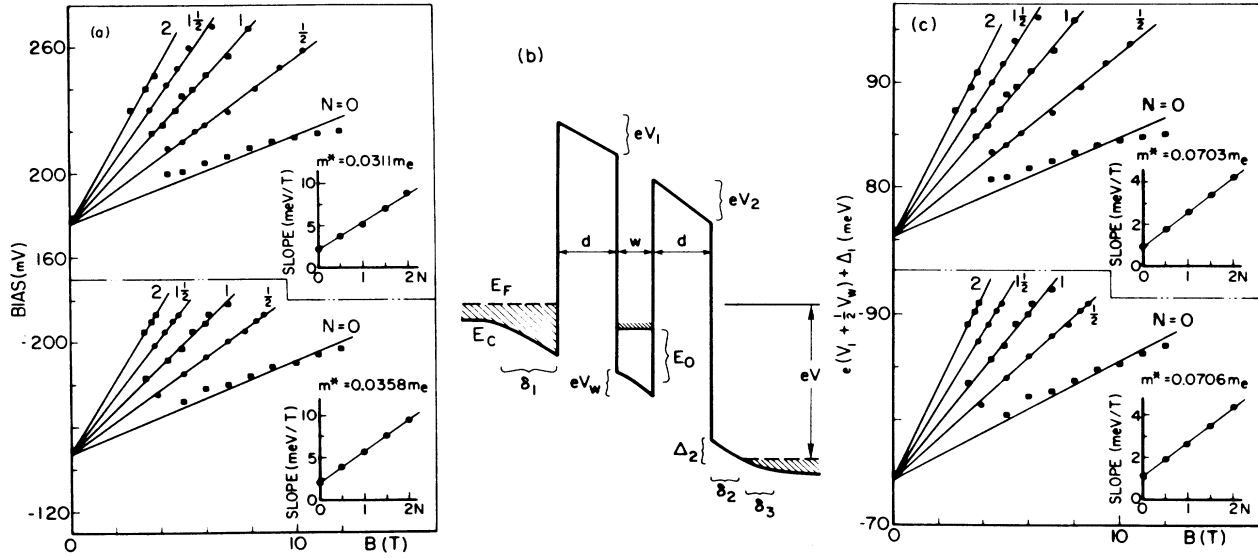


FIG. 3. (a) Positions of the maxima (squares) and the minima (circles) in the differential conductance for both polarities of V . Most of the points are the average of the extrema from dI/dV vs V and dI/dV vs B dependences. The lines are the result of a least-squares fit with the constraint that the $B=0$ intercepts must match. The slopes of the lines, divided by $2/e$ are plotted vs Landau index N in the insets. The least-squares fits shown in the insets give m^* . (b) The CB energy diagram of a DBRTS under bias. Δ_1 and δ_1 are the parameters of the accumulation layer in the emitter; Δ_2 , δ_2 , and δ_3 describe the depletion layer in the collector. The electrostatic potential drops across the emitter barrier, the well and the collector barrier are, respectively, V_1 , V_w , and V_2 . The rest of the notation is explained in the text. The hatching shows the electron occupation. (c) Same as (a), but instead of V is the shift of the bottom of the subband in the well relative to the emitter E_F , $e(V_1 + \frac{1}{2} V_w) + \Delta_1$, calculated as described in the text.

is produced by all the extra electrons in the accumulation layer we can approximate

$$\sigma \approx eN(E_F)\Delta_1\delta_1, \quad (5)$$

where $N(E_F)$ is the density of states at Fermi energy. If we neglect the penetration of the tails of the wave function of the electrons in the well into the barriers, Gauss's law gives

$$V_w/w = V_1/d + (2\pi/\epsilon)\Sigma, \quad (6)$$

and

$$V_2 = V_1 + (4\pi/\epsilon)\Sigma d. \quad (7)$$

The Poisson equation for the δ_2 region of the depletion

layer can be solved easily and gives

$$\Delta_2/e = V_2\delta_2/d - (2\pi/\epsilon)eN_D\delta_2^2. \quad (8)$$

The δ_3 region of the depletion layer presents the same computational difficulty as the accumulation layer; therefore, we used a similar simplification with the linearly changing electrostatic potential, which gives

$$\delta_3 \approx \delta_2 E_F / \Delta_2, \quad (9)$$

and

$$\sigma + \Sigma \approx eN_D(\delta_2 + \frac{1}{2}\delta_3). \quad (10)$$

The areal charge density Σ is given by Eq. (1) with T_2 calculated in the following quasiclassical approximation:¹²

$$T_2 \approx 16 \frac{E_0}{U} \left(1 - \frac{E_0}{U}\right) \exp \left(- \frac{4d(2m^*)^{1/2}}{3\hbar e V_2} \left[(U - E_0 - \frac{1}{2}eV_w)^{3/2} - (U - E_0 - eV_2 - \frac{1}{2}eV_w)^{3/2} \right] \right), \quad (11)$$

where U is the $\text{Al}_x\text{Ga}_{1-x}\text{As}/\text{GaAs}$ CB edge discontinuity.

The self-consistent transcendental system of Eqs. (1)–(11) can be solved numerically using the experimental I - V curve and the material constants.¹³ In order to account for the bias polarity dependence of the I - V characteristic we assumed that, while the outside GaAs electrode has $N_D = 2 \times 10^{17} \text{ cm}^{-3}$, the substrate-side electrode has $N_D = 3 \times 10^{17} \text{ cm}^{-3}$. This assumption is based on the well-known phenomenon of Si diffusion in the molecu-

lar-beam-epitaxy growth direction, the diffusion in $\text{Al}_x\text{Ga}_{1-x}\text{As}$, however, being much slower than in GaAs.¹⁴ The value of $3 \times 10^{17} \text{ cm}^{-3}$ was found to equate the values of E_0 obtained from the fits for both polarities of V , as discussed in the next paragraph.

Having solved the equations for a bias V , we calculate the energy shift of the bottom of the subband in the well relative to the emitter E_F at this bias $e(V_1 + \frac{1}{2} V_w) + \Delta_1$. These energy shifts for the data of Fig. 3(a) are plotted in

Fig. 3(c). A least-squares fit gives $m^* = 0.070m_e$. This value is $\sim 5\%$ greater than m^* in bulk GaAs due to the nonparabolicity of the CB and is in excellent agreement with the cyclotron resonance results.¹⁵ The $B=0$ intercepts of the fits in Fig. 3 should give E_0 , and indeed, they agree very well with the calculated¹² value of 75 meV. The model also gives very reasonable values for the biases corresponding to the current threshold and the current valley: 175 and 420 mV, respectively, for the positive and 160 and 390 mV for the negative polarity.

In conclusion, we note that in our energy diagram [Fig. 3(b)] we assumed that upon doping, CB edge E_c moves down relative to the CB bottom in the undoped well, rather than that the E_F moves up. This assumption is consistent with the limited experimental and theoretical evidence for the energy gap reduction in heavily doped semi-

conductors.¹⁶ If we assume that E_c is aligned in all GaAs regions of the unbiased device, our model gives somewhat worse values for m^* , E_0 , and E_F . The band bending due to the residual doping of the barriers and the well is estimated to produce a negligibly small shift of the subband bottom in the well relative to E_F .¹⁰

Note added. The electron-electron scattering in the well may provide the mechanism destroying the Fabry-Perot interference in DBRTS's. It tends to thermalize the "initial" distribution of tunneling electrons in a very short time. For $n_w \sim 1 \times 10^{11} \text{ cm}^{-2}$ the electron-electron scattering is faster than 10^{-13} sec .¹⁷

The authors acknowledge discussions with H. Morkoç. The work at Princeton is supported by the U.S. Army Research Office.

- ¹T. J. Schewchuk, P. C. Chapin, P. D. Coleman, W. Kopp, R. Fisher, and H. Morkoç, *Appl. Phys. Lett.* **46**, 508 (1985); E. E. Mendez, W. I. Wang, B. Ricco, and L. Esaki, *ibid.* **47**, 415 (1985); T. C. L. G. Sollner, P. E. Tannenwald, D. D. Peck, and W. D. Goodhue, *ibid.* **45**, 1319 (1984); T. C. L. G. Sollner, W. D. Goodhue, P. E. Tannenwald, C. D. Parker, and D. D. Peck, *ibid.* **43**, 588 (1983).
- ²H. Morkoç, J. Chen, U. K. Reddy, T. Henderson, and S. Luryi, *Appl. Phys. Lett.* **49**, 70 (1986).
- ³S. Luryi, *Appl. Phys. Lett.* **47**, 490 (1985).
- ⁴Cf. E. E. Mendez, L. Esaki, and W. I. Wang, *Phys. Rev. B* **33**, 2893 (1986); T. W. Hickmott, *ibid.* **32**, 6531 (1985).
- ⁵R. Tsu and L. Esaki, *Appl. Phys. Lett.* **22**, 562 (1973); B. Ricco and M. Ya. Azbel, *Phys. Rev. B* **29**, 1970 (1984).
- ⁶For clarity we consider only the lowest subband.
- ⁷V. J. Goldman, D. C. Tsui, J. E. Cunningham, and W. T. Tsang, *J. Appl. Phys.* **61**, 2693 (1987).
- ⁸The bias polarity is with respect to the substrate.
- ⁹This picture does not take explicitly into consideration the Landau quantization of the electronic states in the emitter nor does it consider the B dependence of the emitter E_F . These effects, however, are relatively small except in the extreme

quantum limit ($\hbar\omega_c > E_F$), due, in part, to the substantial energy broadening in the heavily doped emitter.

- ¹⁰Cf. T. W. Hickmott, P. M. Solomon, R. Fisher, and H. Morkoç, *J. Appl. Phys.* **57**, 2844 (1985).
- ¹¹See, e.g., T. Ando, A. B. Fowler, and F. Stern, *Rev. Mod. Phys.* **54**, 437 (1982).
- ¹²Cf. I. I. Goldman and V. D. Krivchenkov, *Problems in Quantum Mechanics* (Pergamon, New York, 1961), Chap. 2.
- ¹³We use $\epsilon = 12.7$, $U = 0.320 \text{ eV}$, and other parameters as given in the text.
- ¹⁴K. Inoue, H. Sakaki, and J. Yoshio, *Appl. Phys. Lett.* **46**, 973 (1985), and references therein.
- ¹⁵M. J. Chou and D. C. Tsui, in *Layered Structures, Epitaxy, and Interfaces*, edited by J. H. Gibson and L. R. Dawson, Materials Research Society Symposia Proceedings, Vol. 37 (Materials Research Society, Pittsburgh, 1985), p. 7.
- ¹⁶See, e.g., B. I. Shklovskii and A. L. Efros, *Electronic Properties of Doped Semiconductors* (Springer-Verlag, New York, 1984), Chap. 12.
- ¹⁷C. H. Yang, J. M. Carlson-Swindle, S. A. Lyon, and J. M. Worlock, *Phys. Rev. Lett.* **55**, 2359 (1985).